

## Electronic Supplementary Information for

### **Probing eumelanin photoprotection using a catechol:quinone heterodimer model system**

Christopher Grieco, Jennifer M. Empey, Forrest R. Kohl, Bern Kohler\*

Department of Chemistry and Biochemistry, The Ohio State University, 100 West 18th Avenue, Columbus, Ohio 43210, United States

#### **Table of Contents**

S.1	Additional FTIR spectra . . . . .	2
S.2	Additional UV-Vis spectra . . . . .	4
S.3	Additional UV-Vis-NIR transient absorption spectra and target analysis . . . . .	8
S.4	References . . . . .	15

## S.1 Additional FTIR spectra

Fig. S1 shows the concentration-dependent FTIR spectra of cyclohexane solutions of 3,5-di-*t*-butyl-*o*-quinone (Q) and 3,5-di-*t*-butylcatechol (C). These solutions serve as control samples for the Q+C mixtures presented in the main text.

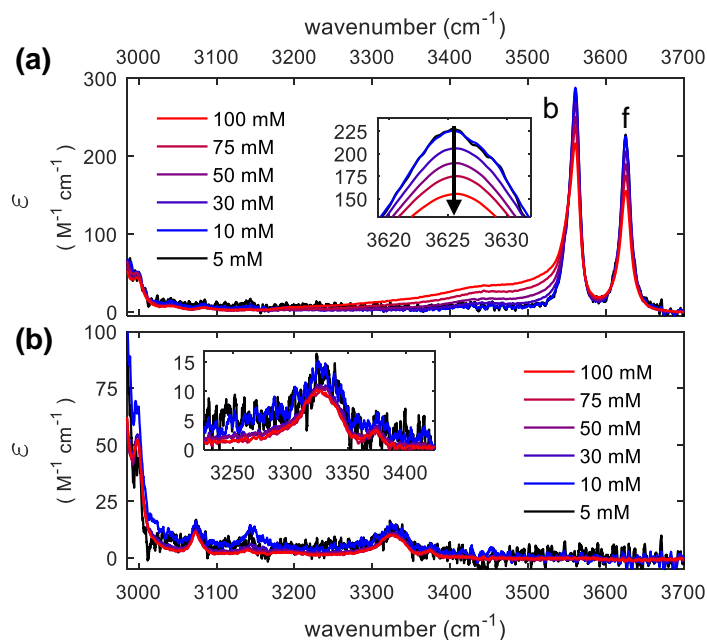


Fig. S1 Concentration-dependent FTIR spectra for cyclohexane solutions of (a) C and (b) Q. The peaks are labeled as free-OH (f) and intramolecularly bonded-OH (b).  $\epsilon$  is the molar absorption coefficient.

The 3450  $\text{cm}^{-1}$  peak in the C spectra indicates the presence of homodimers, which are readily detected for concentrations above 30 mM. The intensity of the free O-H band (f) at 3626  $\text{cm}^{-1}$  in the 30 mM solution decreases by 9.5% relative to that of the 5 mM solution (Fig. S1a, inset), revealing that 9.5% of the molecules form homodimers in the 30 mM sample. Because this decrease is significantly lower than the decrease of 45% of free C molecules in the Q+C solution due to heterodimer formation, the association of two C molecules must be much weaker than the association of C with Q. Therefore, homodimer formation was neglected for Q+C mixtures containing  $\leq 30$  mM C. The weak peaks at 3326 and 3375  $\text{cm}^{-1}$  in the FTIR spectra of Q (Fig. S1b and inset) are assigned to overtones of the C=O stretching modes of Q.

The homodimers in C solutions and heterodimers in Q+C mixture solutions were quantified using a procedure reported previously for 4-*t*-butylcatechol solutions.<sup>1</sup> The fraction of monomers ( $f_{\text{mon}}$ ) in each solution at equilibrium was estimated from eq. S1,

$$f_{\text{mon}} = \frac{\epsilon_c^{3626 \text{ cm}^{-1}}}{\epsilon_{5 \text{ mM, C only}}^{3626 \text{ cm}^{-1}}} \quad (\text{eq. S1})$$

In eq. S1,  $\epsilon_c^{3626 \text{ cm}^{-1}}$ , the apparent molar absorption coefficient (calculated as the absorbance divided by the product of the path length and the initial concentration,  $c$ , of the catechol component) measured at  $3626 \text{ cm}^{-1}$  (free O-H band) is divided by  $\epsilon_{5 \text{ mM}, \text{C only}}^{3626 \text{ cm}^{-1}}$ , the molar extinction coefficient of the 5 mM C solution measured at the same wavenumber. The 5 mM C solution is assumed to contain only uncomplexed C monomers. This assumption is supported by the observation that the molar absorption coefficient of the  $3626 \text{ cm}^{-1}$  peak is the same for the 5 mM and 10 mM solutions.

The concentration of C monomers remaining in solution,  $[C]$ , was then calculated as,

$$[C] = f_{\text{mon}}[C]_{\text{init}}, \quad (\text{eq. S2})$$

where  $[C]_{\text{init}}$  is the initial concentration of C molecules. The fraction of monomers consumed ( $f_{\text{consumed}}$ ) to form either homodimers or heterodimers is given by.

$$f_{\text{consumed}} = 1 - f_{\text{mon}}. \quad (\text{eq. S3})$$

The fraction of monomers consumed in solutions of C and Q+C mixtures is graphed in Fig. S2.

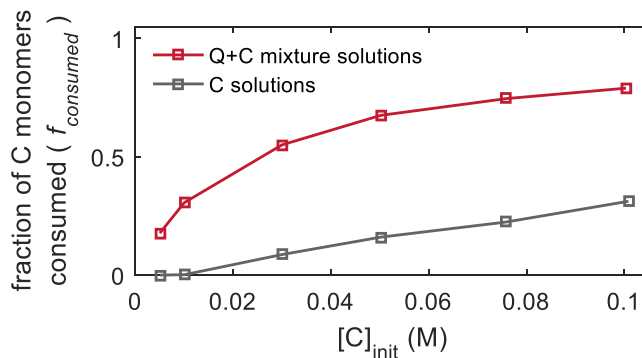


Fig. S2 Fraction of C monomers consumed in cyclohexane solutions of C and Q+C as a function of the initial C concentrations.

For the Q+C solutions, the fraction of monomers consumed was assumed to equal the fraction of Q:C heterodimers present based on the neglect of C:C homodimer formation.

## S.2 Additional UV-Vis spectra

The equimolar mixture of Q and C in cyclohexane (30 mM each) used in transient absorption experiments consists contains an equilibrium mixture of Q and C monomers and Q:C heterodimers, as discussed in the main text. To obtain the spectrum of the Q:C heterodimer ( $A_{Q:C}$ ) from the UV-Vis spectrum of the Q+C solution ( $A_{Q+C}$ ), the contributions by the Q and C monomers were first determined. We assume that Beer's law is obeyed and that the total absorbance is given by the sum of the absorbances of the three species present,

$$A_{Q+C} = A_Q + A_C + A_{Q:C}, \quad (\text{eq. S4})$$

where  $A_Q$  and  $A_C$  are the absorbance contributions from the Q and C monomers, respectively. The fraction of C (and Q) monomers in the equimolar mixture of Q+C was determined from the FTIR spectrum as discussed above. The absorbance spectra of Q and C monomers in cyclohexane (each at 30 mM),  $A_{Q,30 \text{ mM}}$  and  $A_{C,30 \text{ mM}}$ , respectively, were measured under identical conditions as the mixture, and these were scaled to obtain  $A_Q$  and  $A_C$  using eqs. S5 and S6,

$$A_C = f_{\text{mon}} \cdot A_{C,30 \text{ mM}} \quad (\text{eq. S5})$$

$$A_Q = f_{\text{mon}} \cdot A_{Q,30 \text{ mM}}, \quad (\text{eq. S6})$$

where  $f_{\text{mon}}$  is from eq. S1. The absorbance contribution from Q:C heterodimers ( $A_{Q:C}$ ) was then obtained from eq. S4.

Using Beer's law, the absorbances of Q and C were used to calculate the molar absorption coefficient of each as a function of wavelength (Fig. S3). Finally, the molar absorption coefficient of the Q:C heterodimer (purple curve, Fig. S3) was calculated from the concentration of Q:C heterodimers determined using eq. 2 from the main text and the absorbance determined using eq. S4. The path length used for recording UV-Vis spectra of these solutions was 100  $\mu\text{m}$ .

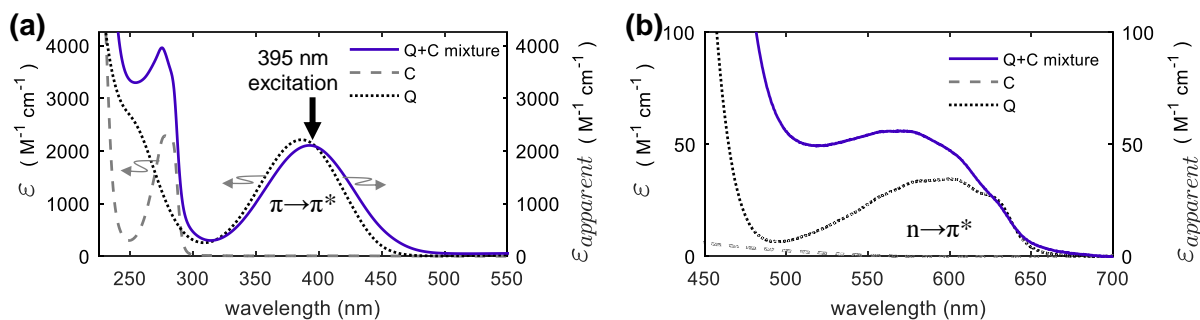


Fig.S3 UV-Vis spectra for cyclohexane solutions of Q, C, and a equimolar mixture of Q+C, in which the initial monomer concentrations were 30 mM. The  $\pi \rightarrow \pi^*$  and  $n \rightarrow \pi^*$  transitions are highlighted in (a) and (b), respectively.  $\epsilon_{\text{apparent}}$  is the apparent absorption coefficient, and  $\epsilon$  is the molar absorption coefficient.

The UV-Vis spectrum of the Q:C heterodimer in cyclohexane solution isolated in this manner is displayed again by the pink curve in Fig. S4. For comparison, the normalized absorption spectra of the Q monomer measured in cyclohexane, ethanol, and 2-propanol are also shown in this figure.

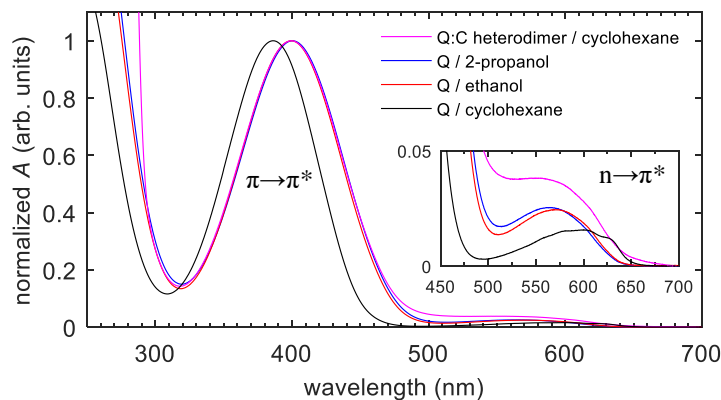


Fig.S4 Comparison of the UV-Vis spectrum of cyclohexane solutions of Q monomers and Q:C heterodimers with Q monomers in alcohols.

Note that the  $\pi \rightarrow \pi^*$  and  $n \rightarrow \pi^*$  peak positions of the Q:C heterodimer in cyclohexane solution occur at nearly the same wavelengths as the corresponding peaks of the Q monomer measured in the two alcohol solvents.

The UV-Vis spectra for 5 mM solutions of Q in various solvents are shown in Fig. S5. Generally, the  $\pi \rightarrow \pi^*$  peak redshifts and the  $n \rightarrow \pi^*$  peak blue shifts upon increasing solvent polarity. The peak centers (in wavenumbers) are well correlated by the Gutmann acceptor number<sup>2, 3</sup> for the solvents tested (cyclohexane, trimethylamine, diethyl ether, tetrahydrofuran, benzene, pyridine, acetonitrile, chloroform, 2-propanol, ethanol, and methanol, see Fig. S5). We conclude that solvatochromism is responsible for the observed shifts. Such a linear correlation is reminiscent of that observed in benzophenone.<sup>4</sup>

The deconvoluted peak centers for pure Q:C heterodimers presented in Fig. 2b in the main text are 399.5 nm and 567 nm for the  $\pi \rightarrow \pi^*$  and  $n \rightarrow \pi^*$  peaks, respectively. Using these values, one predicts from the linear correlation curves obtained for protic solvents (see Fig. S6) Gutmann acceptor numbers for C of 35.3 and 35.8 from the  $\pi \rightarrow \pi^*$  and  $n \rightarrow \pi^*$  peaks, respectively. These values fall between those of 2-propanol and ethanol.

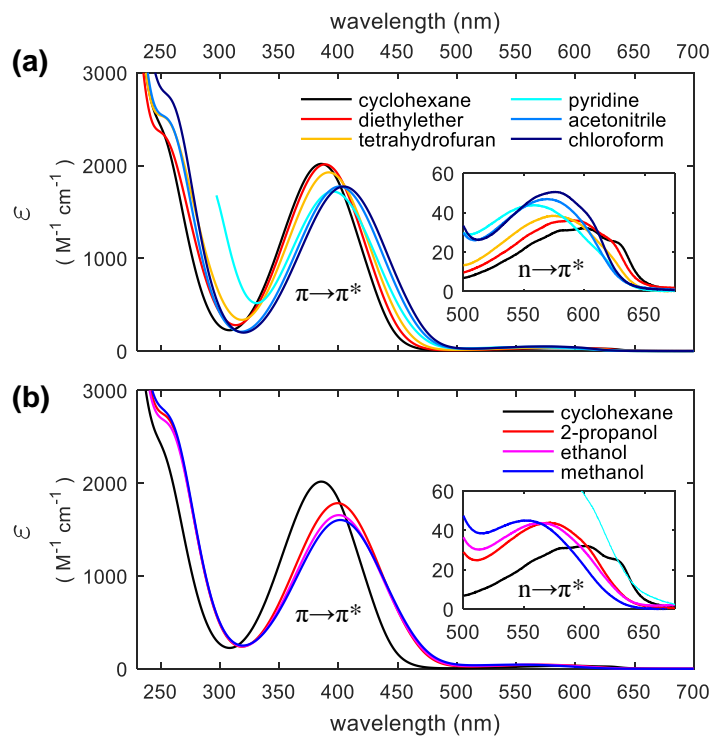


Fig. S5 Solvent-dependent UV-Vis spectra of 5 mM solutions of Q in (a) aprotic and (b) protic solvents. The cyclohexane solution spectrum is shown in (b) for reference.

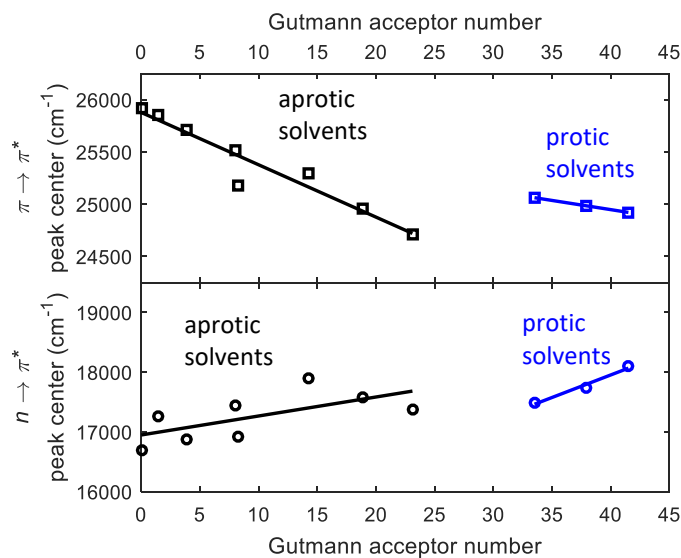


Fig. S6 Correlation of the  $\pi \rightarrow \pi^*$  and  $n \rightarrow \pi^*$  peak centers of Q to the Gutmann acceptor number of the solvent for both aprotic and protic solvents.

The UV-Vis spectra for Q+C solutions in cyclohexane are shown in Fig. S7 as a function of the concentration of C (equal to the concentration of Q). The spectra have been normalized to have the same absorbance at the peak seen between 250 and 300 nm. There is a gradual red shift and blue shift of the  $\pi \rightarrow \pi^*$  and  $\pi \rightarrow \pi^*$  bands, respectively. The peak positions of both bands approach the spectrum of the Q:C heterodimer seen in Fig. 3b of the main text. Additionally, the difference spectra in Fig. S7b show no significant spectral shifts with increasing solution concentration.

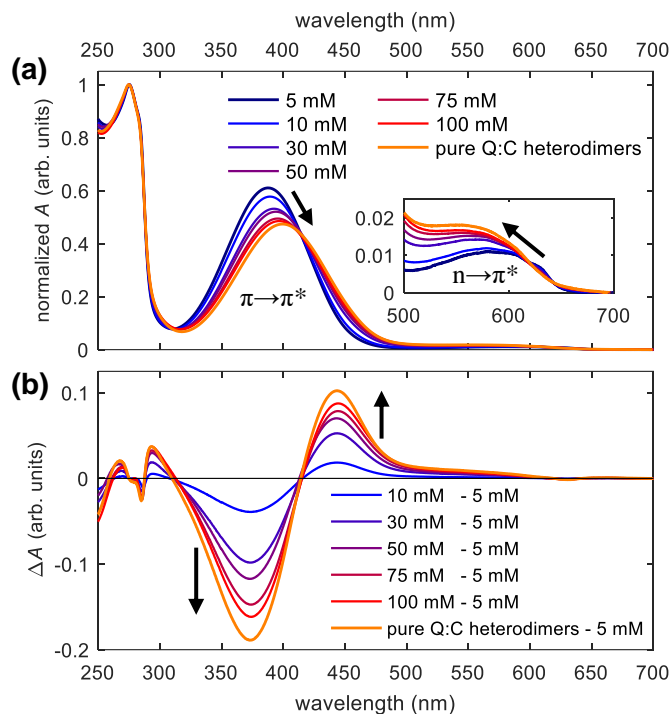


Fig. S7 Concentration-dependent (a) UV-Vis spectra and (b) difference spectra for equimolar solutions of Q+C in cyclohexane. The concentrations listed are the initial concentrations of each component added to the mixture. The pure Q:C heterodimer spectrum is included in (a) for reference.

### S.3 Additional UV-Vis-NIR transient absorption spectra and target analysis

Target analysis of the transient absorption spectrum of the Q monomer in cyclohexane was performed using a sequential kinetic model. The resulting species associated difference spectra (SADS) and their associated decay time constants are shown in Fig. S8. The intersystem crossing pathway follows the El-Sayed rules.<sup>5</sup>

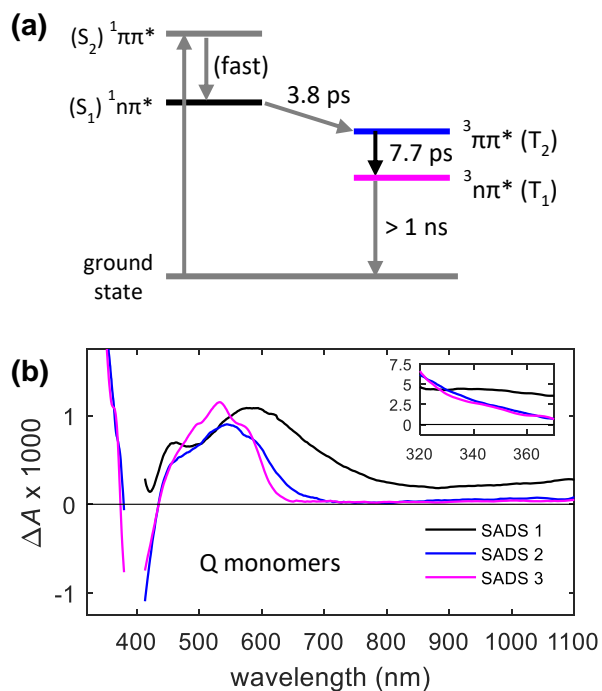


Fig. S8 (a) Sequential kinetic scheme for the excited state pathways of the Q monomer in cyclohexane. (b) Species associated difference spectra (SADS) obtained from target analysis of the transient absorption spectrum recorded for a 30 mM solution of Q in cyclohexane. The colors of the states in (a) match the colors of the spectra.



The transient absorption spectrum for a 30 mM solution of Q in 2-propanol is shown in Fig. S9 and the kinetic traces capturing the  $^1Q^*$  and  $^3Q^*$  dynamics are shown in Fig. S10.

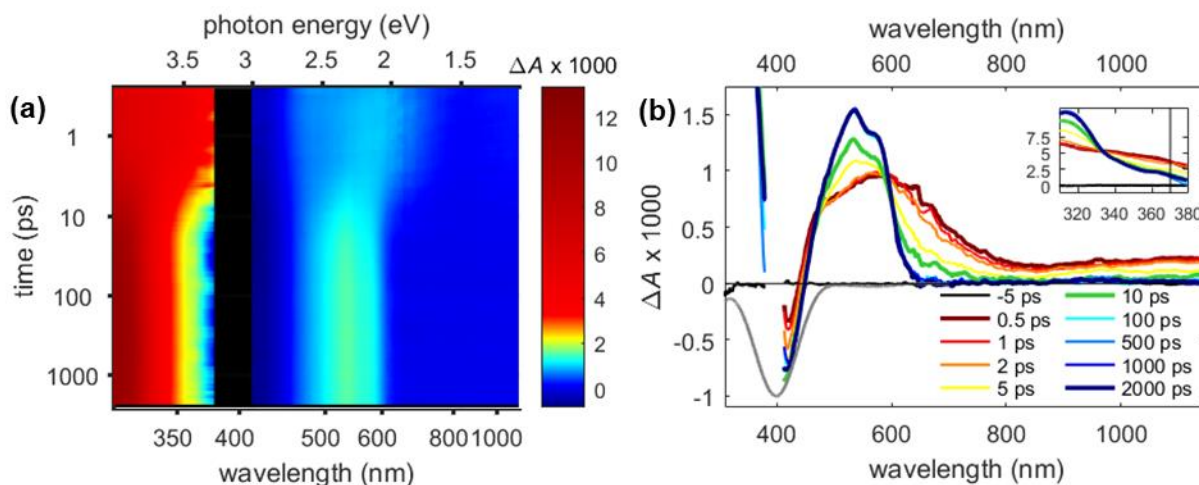


Fig.S9 (a) 2D maps of the transient absorption spectrum of a 30 mM solution of Q in 2-propanol measured using 395 nm excitation. (b) Transient absorption spectra at select time delays. The gray trace is the inverted absorption spectrum. The inset shows the UV portion of the spectra.

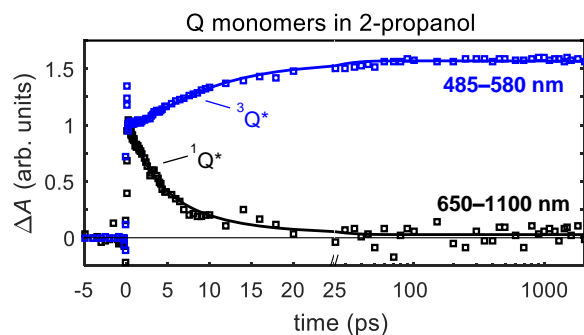


Fig. S10 Transient absorption kinetics averaged over the indicated wavelengths for Q in 2-propanol excited at 395 nm. Solid lines are fits to the data using a branched target model to guide the eye.

Fig. S11a shows the raw transient absorption spectrum for the equimolar mixture of Q and C (30 mM each) in cyclohexane before subtraction of the Q monomer contribution. For comparison, Fig. S11b shows the transient absorption spectrum recorded for a 30 mM solution of C in cyclohexane using the same excitation conditions and path length. No signals were detected in this solution as expected because the C molecules do not absorb at the 395 nm pump wavelength.

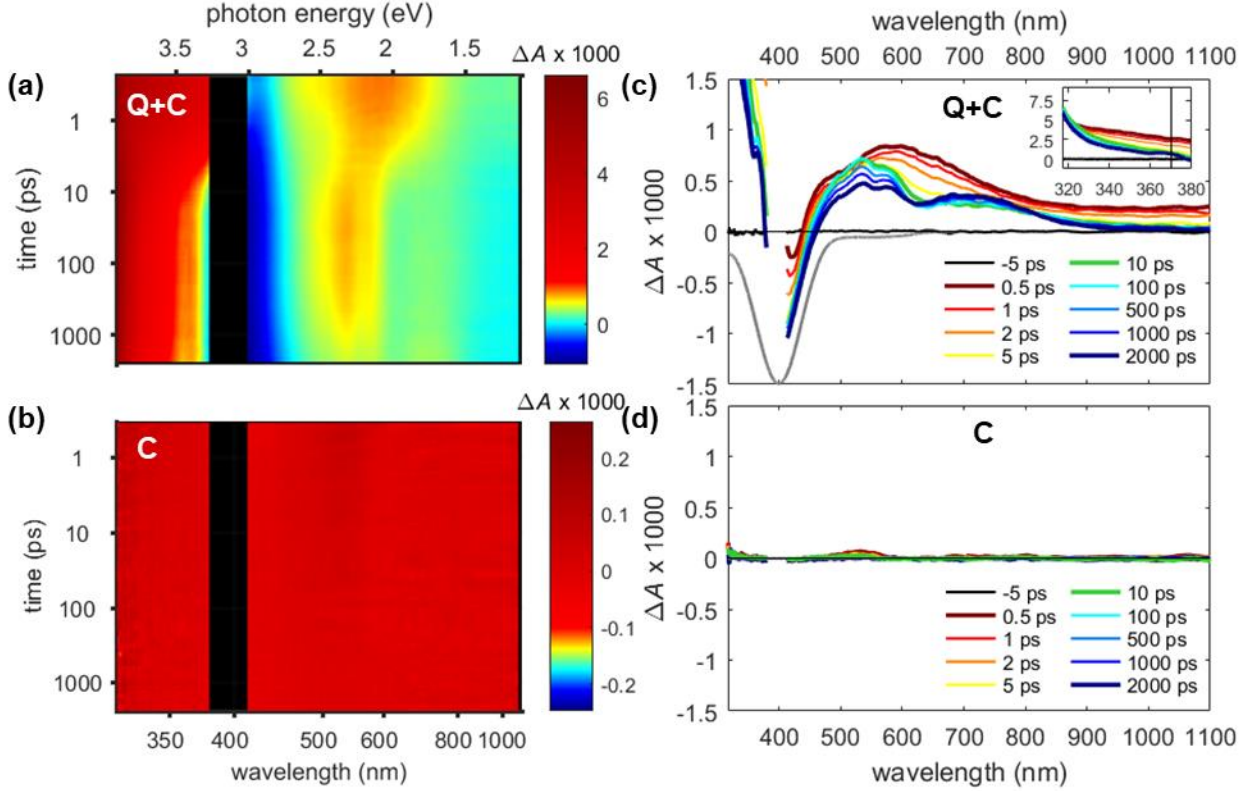


Fig. S11 (a,b) 2D maps of the transient absorption spectrum of (a) a Q+C mixture and (b) C in cyclohexane, both measured using 395 nm excitation. (c,d) Transient absorption spectra at select time delays for (c) the Q+C solution and (d) C solution. The gray traces in (c) and (d) are the inverted absorption spectra of the Q+C and C solutions, respectively. The inset in (c) shows the UV portion of the spectrum for the Q+C mixture. A vertical line at 370 nm is drawn for reference.

The Q+C solution contains Q:C heterodimers in addition to free Q and C monomers. Because the C molecules do not absorb the pump wavelength at 395 nm, a solution of just C produces no transient absorption signals (Fig. S11b and d). Consequently, the transient absorption signals from the Q+C solution contain contributions from just two species: the Q:C heterodimer and the Q monomer. When absorption saturation and multiphoton excitation can be neglected, each component in a mixture of absorbers contributes to the signal in proportion to its contribution to the total absorbance.<sup>6</sup> It is possible to show that the signal from a Q+C solution,  $\Delta A_{Q+C}(t)$ , can be decomposed into signals produced from (hypothetical) solutions containing just Q:C and Q,  $\Delta A'_{Q:C}(t)$  and  $\Delta A'_Q(t)$ , respectively,

$$\Delta A_{Q+C}(t) = \frac{A_{Q:C}}{A} \Delta A'_{Q:C}(t) + \frac{A_Q}{A} \Delta A'_Q(t). \quad (\text{eq. S7})$$

Eq. S7 is valid when all of the transient absorption signals are recorded from solutions having the identical pump-wavelength absorbance  $A$ , using pump pulses with identical incident fluence.  $\Delta A'_{Q:C}(t)$  is thus the hypothetical transient absorption signal that would have been measured for a hypothetical solution of pure Q:C heterodimers having the same absorbance of 0.629 as the separate Q+C and Q solutions. The components of the total signal measured for the Q+C mixture in eq. S7 can be expressed alternatively as,

$$\Delta A_{Q:C}(t) = \frac{A_{Q:C}}{A} \Delta A'_{Q:C}(t) \quad (\text{eq. S8})$$

$$\Delta A_Q(t) = \frac{A_Q}{A} \Delta A'_Q(t) \quad (\text{eq. S9})$$

These components,  $\Delta A_{Q:C}(t)$  and  $\Delta A_Q(t)$ , the sum of which yields the measured transient absorption signal of the Q+C solution, are what are listed in eq. 4 in the main text. Finally, the Q:C heterodimer population in the Q+C solution has absorbance  $A_{Q:C}$  and the Q monomer population in the same solution has absorbance  $A_Q$ . Because C does not absorb at the pump wavelength,

$$A_{Q+C} = A_{Q:C} + A_Q. \quad (\text{eq. S10})$$

The values of  $A_{Q:C}$  and  $A_Q$  at 395 nm obtained from the decomposition in Fig. 2b in the main text are 0.341 and 0.288, respectively. Using these values and the signal measured for a solution of Q only in Fig. 3a,c, eqns. S7–S10 were used to solve for  $\Delta A_{Q:C}(t)$ , which is shown in Fig. 3b,d in the main text. Further examples of this decomposition procedure are shown in Fig. S12.

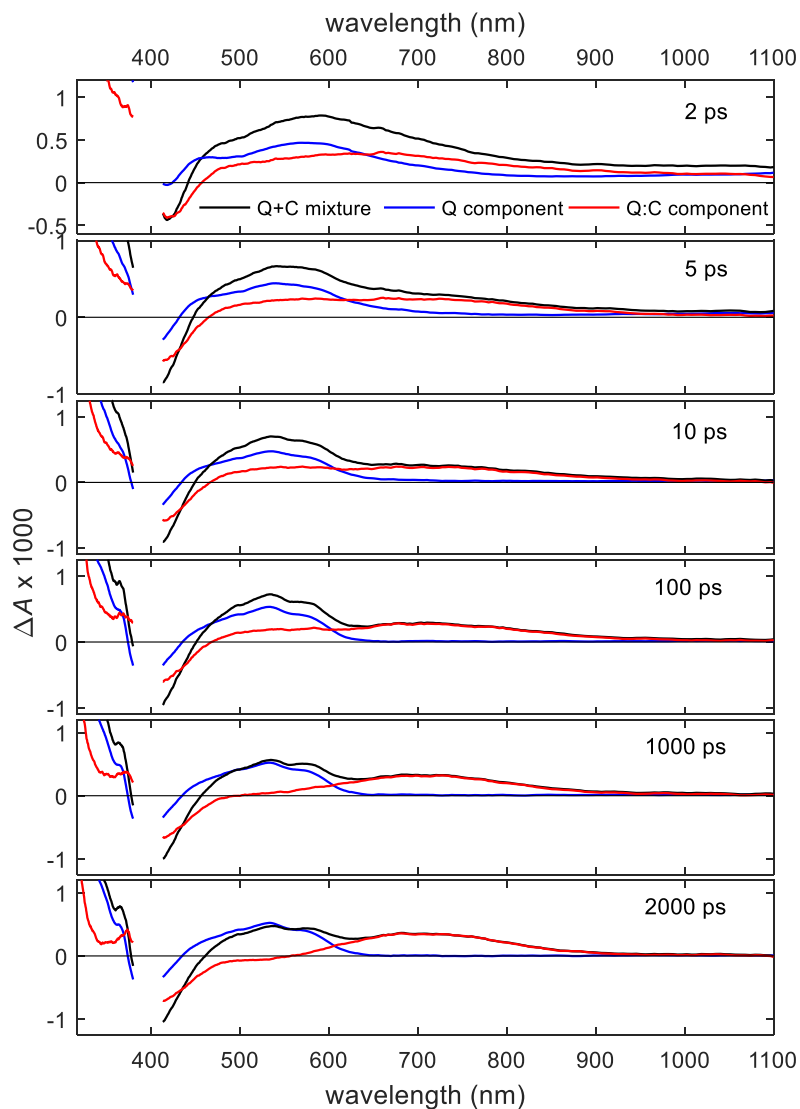


Fig. S12 Illustration of the subtraction procedure for obtaining the transient absorption signal components arising from Q and from the Q:C heterodimer at the indicated time delays. The black traces correspond to  $\Delta A_{Q+C}(t)$ , the blue traces correspond to  $\Delta A_Q(t)$ , and the red traces correspond to  $\Delta A_{Q:C}(t)$ .

The transient absorption spectrum of the Q:C heterodimers in cyclohexane is presented at several other time delays to better highlight the spectral dynamics presented in the main text. The spectra are presented on both the early picosecond timescale (Fig. S13a) and the hundreds of picoseconds timescale (Fig. S13b). The former spectra highlight the formation of neutral semiquinone (SQ) radicals and triplet ( $^3Q^*$ ) states, both formed from singlet ( $^1Q^*$ ) states of the quinone. The latter spectra, which are normalized to the SQ radical peak at 710 nm, highlight the dynamic peak narrowing.

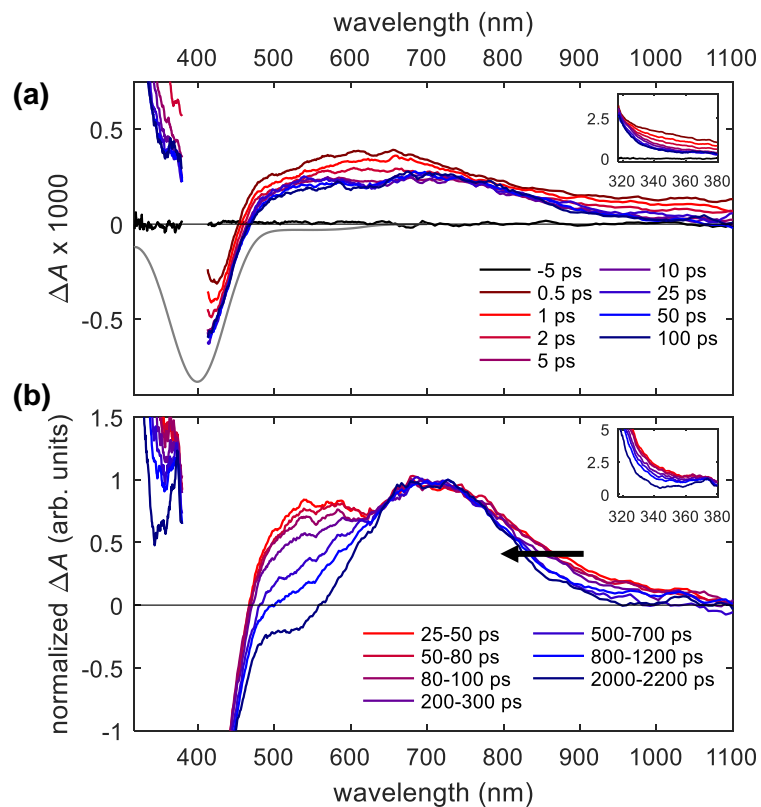


Fig. S13 Transient absorption spectra for Q:C heterodimers in cyclohexane shown for (a) several time delays prior to decay of the  $^3Q^*$  states, and (b) averaged over several time ranges to highlight the narrowing of the 710 nm peak. Note that the spectra in (b) are normalized to the peak at 710 nm. The insets in (a) and (b) show the UV portion of the spectra.

Fig. S14 shows the target analysis model and the SADS for the Q:C heterodimer.

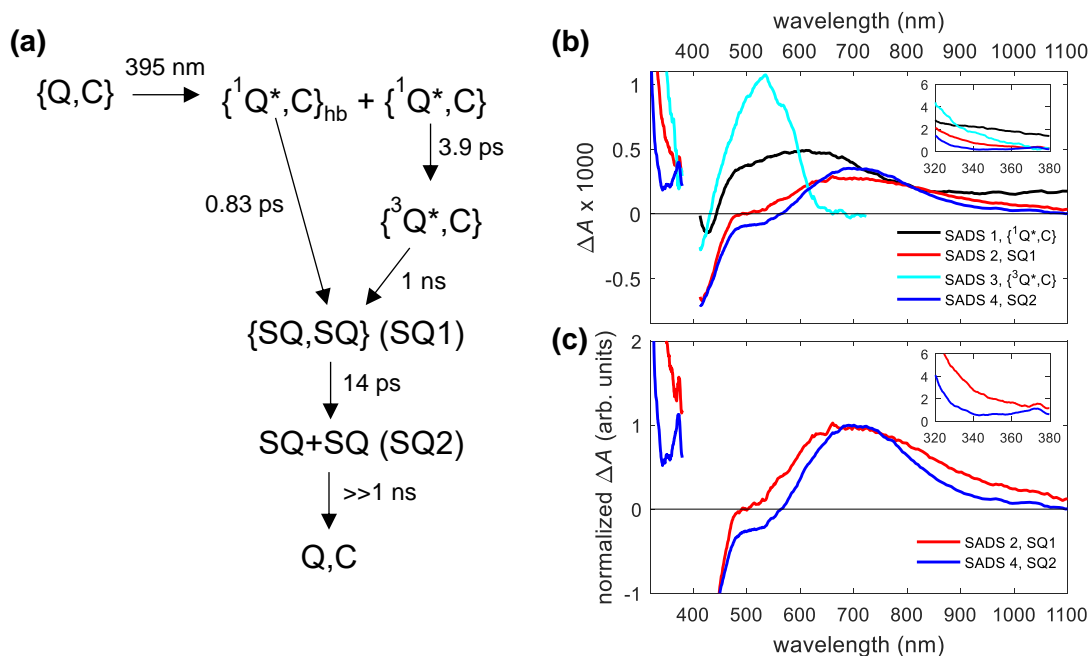


Fig. S14 (a) Kinetic model for Q:C heterodimers in cyclohexane, including time constants obtained from target analysis of the transient absorption spectra. Curvy brackets indicate contact pairs and hb is hydrogen bonded. (b) Species associated difference spectra (SADS) obtained from target analysis. (c) Normalized SADS of the semiquinone radical pairs. The insets in (b) and (c) show the UV portion of the spectra.

Fig. S15 shows the transient absorption spectrum for the Q monomer in cyclohexane measured from visible to near-IR wavelengths. Peaks appear at photon energies approximately equal to the transition energies predicted in the main text (Fig. 3c and lines in Fig. S15a), which correspond to the  $\pi \rightarrow n$  and  $n \rightarrow \pi^*$  transitions of the  $^1n\pi^*$  state of Q.

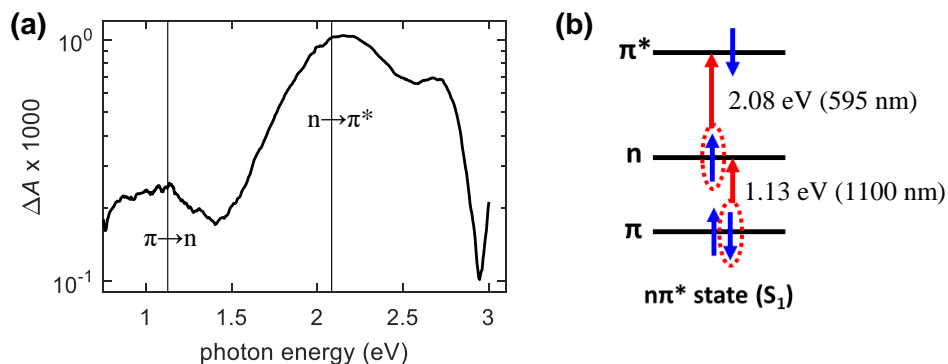


Fig. S15 (a) Transient absorption spectrum of a 30 mM solution of Q in cyclohexane at 500 fs following photoexcitation at 395 nm. The data are plotted on a logarithmic vertical axis. Vertical lines at 1.13 eV (1100 nm) and 2.08 eV (595 nm) correspond to the transition energies predicted in the main text, which are reproduced in the energy level diagram in (b).

## S.4 References

1. C. Grieco, F. R. Kohl, Y. Zhang, S. Natarajan, L. Blancafort and B. Kohler, *Photochem Photobiol*, 2018, DOI: 10.1111/php.13035.
2. U. Mayer, V. Gutmann and W. Gerger, *Monatshefte für Chemie*, 1975, **106**, 1235-1257.
3. M. J. Kamlet, J. M. Abboud, M. H. Abraham and R. W. Taft, *J. Org. Chem.*, 1983, **48**, 2877-2887.
4. V. Ravi Kumar, C. Verma and S. Umapathy, *J Chem Phys*, 2016, **144**, 064302.
5. M. A. El-Sayed, *The Journal of Chemical Physics*, 1963, **38**, 2834.
6. B. Kohler, in *Ultrafast Dynamics at the Nanoscale: Biomolecules and Supramolecular Assemblies*, eds. I. Burghardt and S. Haacke, Pan Stanford Publishing Pte Ltd, Singapore, 2017, pp. 3-64.